

An automated thermal relaxation calorimeter for operation at low temperature ($0.5 \text{ K} < T < 10 \text{ K}$)

S BANERJEE, M W J PRINS, K P RAJEEV and
A K RAYCHAUDHURI

Department of Physics, Indian Institute of Science, Bangalore 560012, India

MS received 16 April 1992

Abstract. We describe an automated calorimeter for measurement of specific heat in the temperature range $10 \text{ K} > T > 0.5 \text{ K}$. It uses sample of moderate size (100-1000 mg), has a moderate precision and accuracy (2%-5%), is easy to operate and the measurements can be done quickly with He⁴ economy. The accuracy of this calorimeter was checked by measurement of specific heat of copper and that of aluminium near its superconducting transition temperature.

Keywords. Relaxation calorimeter; specific heat; low temperature.

PACS No. 07.20

1. Introduction

Specific heat of a solid (C_p) is an important quantity. Often the specific heat at low temperatures ($T < 10 \text{ K}$) are needed to fix both the Debye temperature (θ_D) and the density of state at Fermi level ($N(\epsilon_F)$). In addition, presence of other low energy excitations in a solid also show up in C_p at $T < 10 \text{ K}$. For example in glasses and amorphous solids, an extra linear specific heat term often shows up for $T < 2 \text{ K}$. In magnetic solids low temperature transitions show clear manifestations in the specific heat. For laboratories involved in solid state physics, calorimetry at low temperatures ($T < 10 \text{ K}$) is an extremely useful experimental tool (Lakshmikummar and Gopal 1981). The purpose of this paper is to present the description of a simple calorimeter operating in the temperature range $0.5 \text{ K} < T < 10 \text{ K}$. The calorimetry in this temperature range is developed and is also well documented (Stewart 1983). The systems described range from complicated to simple, though the basic principle often remains the same. The complexity of the calorimetry depends on the magnitude of the heat capacities to be studied and the temperature range. For instance, calorimetry on small samples ($\sim 1-10 \text{ mg}$) or thin films need higher precision as well as accuracy. The detection of small C_p changes associated with a phase transition will call for high precision but small compromise may be made on the accuracy. Presence of magnetic field often introduces complexity arising out of thermometer calibration.

The calorimeter described here depends on the well-known principle of relaxation calorimetry (Bachmann *et al* 1972; Schultz 1974; De Puydt and Dahlberg 1986; Dutzi *et al* 1988). However, the details of the implementation and the improvisation contain

new aspects. In this paper we point out these aspects and we wish to provide the necessary details wherever required. The system designed by us has the following features:

- (1) It is simple to build from the design state to the final state, and is based upon commonly available ingredients.
- (2) It employs electronics which are general purpose and are commonly available in advanced laboratories.
- (3) The automation is by using a PC/XT which interface to the instrument via GPIB and uses BASIC or PASCAL for software. The software is flexible enough to cater to user modifications.
- (4) It uses samples of moderate size (100–1000 mg) and has a moderate precision and accuracy (2%–5%).
- (5) The cryogenic system for the calorimeter is based on a simple home-made one shot He³ cryostat. The sample mounting to completion of the experiment takes 12–14 h, needing 10 litres of liquid helium. The quick turn around time facilitates rapid measurements.

Generally, each calorimeter is designed to suit the specific need of the designer. However, it is expected to be general enough to accommodate other users. The calorimeters described here is meant for users who need to measure quickly the C_p of a series of samples with moderate (2%–5%) accuracy and where samples of quantities 100–1000 mg are available.

The paper is divided into five sections. In § 2 we briefly describe the principle. In § 3 we describe the calorimeter, the cryostat and the associated electronics. In § 4 we give the procedure of taking data followed by an evaluation of the calorimeter performance in § 5. The useful details of the software are given in the Appendix.

2. Principle of operation

The basic equation of calorimetry is given as,

$$\dot{Q}_{in} = C(T)\dot{T} + \dot{Q}_{loss} \quad (1)$$

where \dot{Q}_{in} is the power input to the solid of total heat capacity (sample + addenda) $C(T)$ whose temperature T changes at the rate \dot{T} . \dot{Q}_{loss} is the rate of heat loss from the system through conduction, radiation and convection. For adiabatic calorimetry $\dot{Q}_{loss} \approx 0$, and from (1), the temperature rise ΔT of the solid in response to a total heat input ΔQ_{in} gives the total heat capacity

$$C(T) = \frac{\Delta Q_{in}}{\Delta T} \quad (2)$$

At low temperatures, typically below 15 K, when the radiation loss starts becoming negligible nonadiabatic or quasi adiabatic methods (pulsed or relaxation calorimetries) are generally used. Relaxation calorimetry with different modifications can be used for $T < 15$ K. The basic thermal system of our relaxation calorimeter is shown in figure 1. The calorimeter (a sapphire substrate), on which the sample is thermally anchored, is connected by heat link to the base maintained at temperature T_B . The total heat

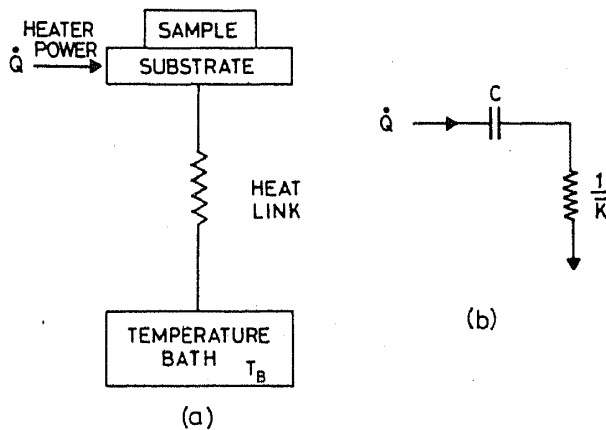


Figure 1. Thermal relaxation method (a) schematic of thermal circuit, and (b) electrical analog.

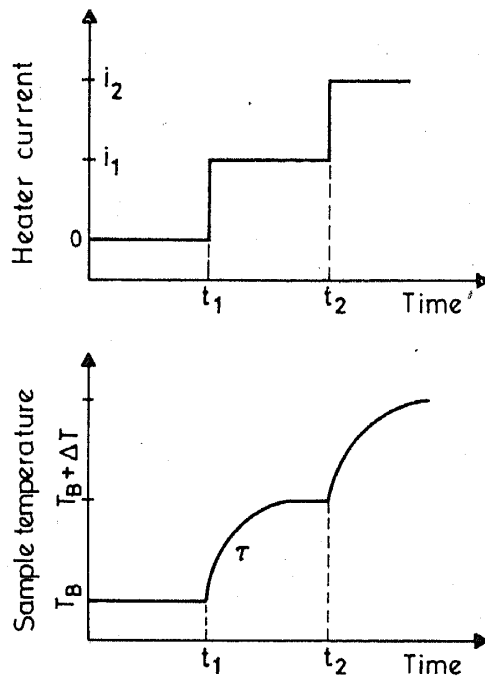


Figure 2. Response of the calorimeter to step heating, $\dot{Q}_{\text{heater}} = I^2 R_H$ where R_H is the resistance of the sample heater.

capacity (sample + substrate) is C and the heat link has a thermal conductance \bar{K} . At zero time, before application of heat, the temperature T of the calorimeter is at the base temperature $T \approx T_B$. [In practice, spurious heat input makes T somewhat larger than T_B . In our cryostat the spurious heat input makes $T \approx 0.6$ K when $T_B \approx 0.45$ K. In the evaluation of C this spurious heat is measured and accounted for]. The heat input to the calorimeter is given by increasing the calorimeter heater current in well defined steps as sketched in figure 2. The response of the calorimeter to step heating is also sketched in figure 2. This is analogous to a capacitor (C) being charged through a resistor ($1/\bar{K}$) (see figure 1). The heat balance equation is given as

$$\dot{Q}_{\text{heater}} = C(T) \dot{T} + \bar{K}(T - T_B) \quad (3)$$

where $\dot{Q}_{in} = \dot{Q}_{heater}$ and $\dot{Q}_{loss} = \bar{K}(T - T_B)$ see (1). The heat loss in this case is mostly through the link of thermal conductance \bar{K} . High vacuum in the calorimeter and low temperatures ensure that other modes contribute very little. In this method we actually measure \dot{Q}_{loss} experimentally.

The temperature rise of the sample (and addenda) are characterized by the thermal time constant $\tau(T)$.

$$\tau(T) = C(T)/\bar{K}(T). \quad (4)$$

The aim of this method is to find $\tau(T)$ from the $(T-t)$ curve and also $\bar{K}(T)$ from \dot{Q}_{loss} measurements so that $C(T)$, the total heat capacity, can be obtained from (4). The temperature rise after the n th step is given as,

$$T(t) = T_{n-1} + \Delta T_n(1 - \exp(-t/\tau_n)) \quad (5)$$

where $\Delta T_n = T_n - T_{n-1}$ is the total temperature rise in the n th step. The time t in (5) is from the time the n th heat pulse is applied. The thermal time constant τ_n refers to the n th step $\tau_n = \tau(\bar{T}_n)$, $\bar{T}_n = (T_n + T_{n-1})/2$. The temperature T_n at the end of n th step is reached for $t \gg \tau_n$. In this method T_n and T_{n-1} (and hence ΔT_n) are experimentally determined directly. τ_n is determined from the recorded $(T-t)$ curve using (5) by nonlinear least square fit.

For $t \gg \tau$, one reaches a steady state so that $\dot{T} \approx 0$. Then from (3), $\bar{K}(T)$ can be determined:

$$\bar{K}(T) = \bar{K}(\bar{T}_n) \equiv \frac{\dot{Q}_{heater}}{(T_n - T_B)} \quad (6)$$

where $\bar{T}_n = (T_n + T_{n-1})/2$. ΔT_n is in the range 0.1–0.3 K. Determination of τ from (5) and \bar{K} from (6) gives C from (4). [\dot{Q}_{heater} is the applied power and the small spurious heat leak into the calorimeter. The spurious heat leak is obtained from the difference in base temperature and lowest substrate temperature (no heat applied)]. $\bar{K}(T)$ in (6) is determined by the total heater power (\dot{Q}_{heater}) and not by the power applied in the n th step. When we write $\bar{K}(T_n)$, we mean the total thermal conductance of the link with the calorimeter held at temperature T_n . [The average temperature of the link $\approx (T_n + T_B)/2$. For our purpose, since $\bar{K}(T_n)$ is directly measured this distinction is not of any consequence].

The description given above refers to heating steps. Analogous description applies to cooling steps also. As a result in this method we can take data during heating as well as cooling.

3. Experimental details

3.1 Calorimeter

The calorimeter consists of a sapphire (single crystal) plate of dimension 12 mm \times 12 mm \times 0.3 mm. The sapphire calorimeter is suspended from the thermal anchor plate (see figure 3) by nylon threads. The thermal anchor plate kept at base temperature T_B is the thermal ground for all leads (heater and thermometer) going to the calorimeter.

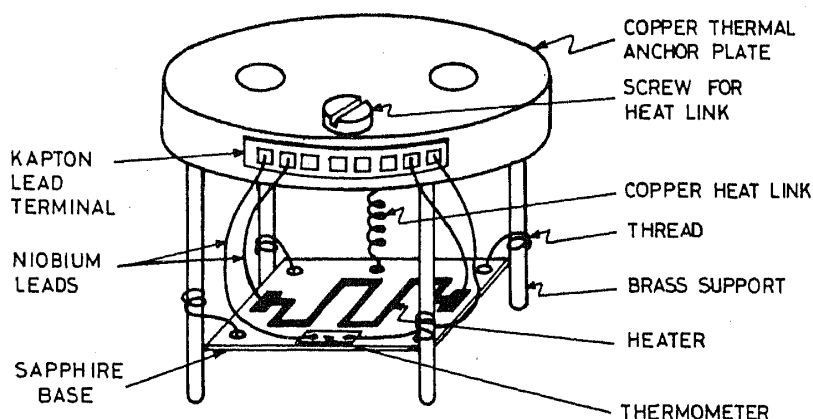


Figure 3. Sample holder with sample platform (sapphire), heater, thermometer, heat link and leads.

One side of the sapphire plate has an evaporated Cr heater of resistance $\sim 2 \text{ k}\Omega$. The same side also has a carbon thermometer. The thermometer is an Allen Bradley resistor (10Ω) which was ground down to around $1/2 \text{ mm}$ or less thickness by polishing it on both sides. The carbon thermometer has a RT resistance of $1.2 \text{ k}\Omega$ and this becomes $6.3 \text{ k}\Omega$ at 0.4 K . The carbon thermometer is mounted on the sapphire calorimeter by little GE 7031 varnish (A better alternative is to evaporate Ge–Au alloy strip on sapphire for use as thermometer. We are currently working on this technique). The leads to the heater and thermometer are made from 75μ superconducting Nb wire. This gives leads of low thermal conductance and extremely high electrical conductance. The use of low thermal conductance Nb leads allow us to tune the thermal link (described below) to proper \bar{K} value by a separate copper wire. The end of the Nb leads have small pieces ($1\text{--}2 \text{ mm}$) of Cu–Ni capillary crimped on to them which serve as soldering lugs. However the operation of the calorimeter is restricted to below T_c of Nb ($\approx 9.6 \text{ K}$). The thermometer is calibrated with all the leads which are actually used, to avoid any uncertainties.

The thermal link of the calorimeter is an important part of the design because this determines the time constant τ . τ should not be too large or too small. If τ is too small, and of the same order as the internal thermal equilibrium time constants of the sample, calorimeter and the thermometer, the $(T - t)$ curve cannot be described by a single time constant τ as in (5). It is important to estimate these times constants realistically before finding a lower bound for τ . The lower bound of τ also has to be compatible with the data conversion rate of the temperature recording device (in our case a lock-in amplifier coupled to a fast recording DMM) at the desired precision ($4\frac{1}{2}$ or $5\frac{1}{2}$ digit). A discussion on time constants can be found elsewhere (Raychaudhuri 1980; Shepherd 1985). The upper limit of τ sets the time to take data. For the measurement of \bar{K} one needs to attain an almost quasi steady state situation ($\dot{T} \approx 0$) between two heating (or cooling) steps. This is possible when the time between steps is much larger than τ . If τ is too large then the wait time becomes too long. This not only increases the data taking time, additional effects due to long term drift of the base temperature etc. comes into play. Also where τ is large, for a given C , \bar{K} is small. When \bar{K} is small (see (6)) \dot{Q}_{heater} is small for the same $(T - T_B)$. This implies that a little heat input can give a larger $(T - T_B)$. In such condition effect of spurious heat inputs becomes more significant.

In our calorimeter τ is kept in the range $1\text{--}2 \text{ s}$ for empty calorimeter and with sample

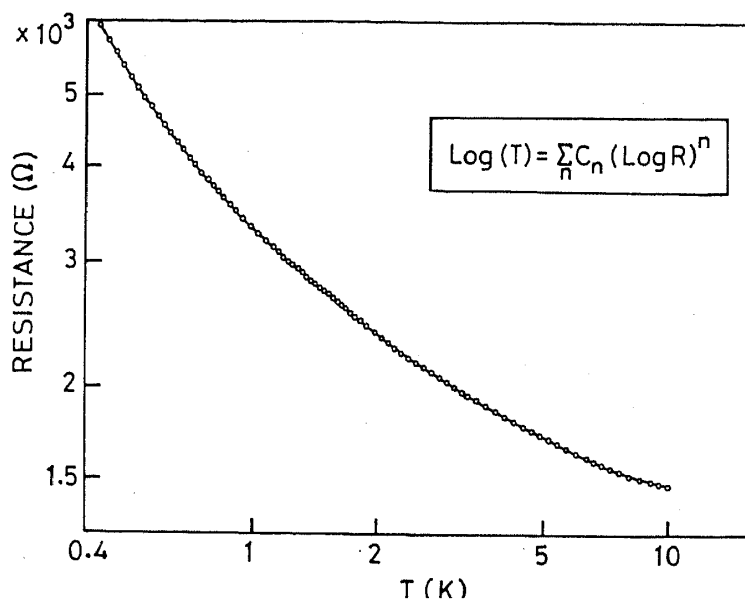


Figure 4. Resistance vs temperature of carbon thermometer and fit from equation (7).

τ is 2–10 s. The heat link is made from gauge #44 copper wire. One end of the link is attached to the thermal anchor and other end to the calorimeter. The length of the link is adjusted to obtain the desired \bar{K} and τ . The total link thermal resistance ($1/\bar{K}$) contains the wire thermal resistance as well as the boundary resistances at the two ends of the wire.

The thermometer on the calorimeter plate is calibrated against the Ge thermometer on the base in a separate run by mounting the calorimeter plate directly on the base. The calibration of the carbon thermometer on the calorimeter is stable from run to run and after few runs the calibration is rechecked for small drifts. We use a polynomial for fitting the ($R - T$) curve. A typical calibration data is shown in figure 4. The polynomial used is

$$\log T = \sum_n C_n (\log R)^n. \quad (7)$$

3.2 Cryostat

The calorimeter temperature base is provided by a simple home made He^3 cryostat. The schematic of cryostat is shown in figure 5(a) and gas handling system in figure 5(b). The vacuum chamber sealed by indium O-ring (diameter 1 mm) is pumped to better than 10^{-5} torr before start of the run and then isolated from the pumping system. The vacuum chamber is surrounded by pumped He^4 kept at 1.5 K. For this we use a 600 l/min sealed pump (Edwards model 2HS40). This cools the inside base to 1.5 K and the He^3 gas (kept in room temperature storage vessel) condenses into the evaporator (volume $\sim 8 \text{ cm}^3$). The total He^3 gas used is ~ 2.25 NTP litre which condenses into liquid of volume $\sim 3 \text{ cm}^3$. After condensation, the He^3 is pumped by a sealed pump through a manifold of varying pumping impedance. The cryostat after pumping on He^3 reaches 0.4 K within 1/2 h. The volume of liquid (3 cm^3) in the evaporator is enough to maintain it at 0.4 K for 4 h under normal heat load. This time is enough to take heating/cooling scan from 0.5 K to 10 K. If the scan needs to be repeated, the He^3 gas can be recondensed and the entire cycle can be repeated within an hour.

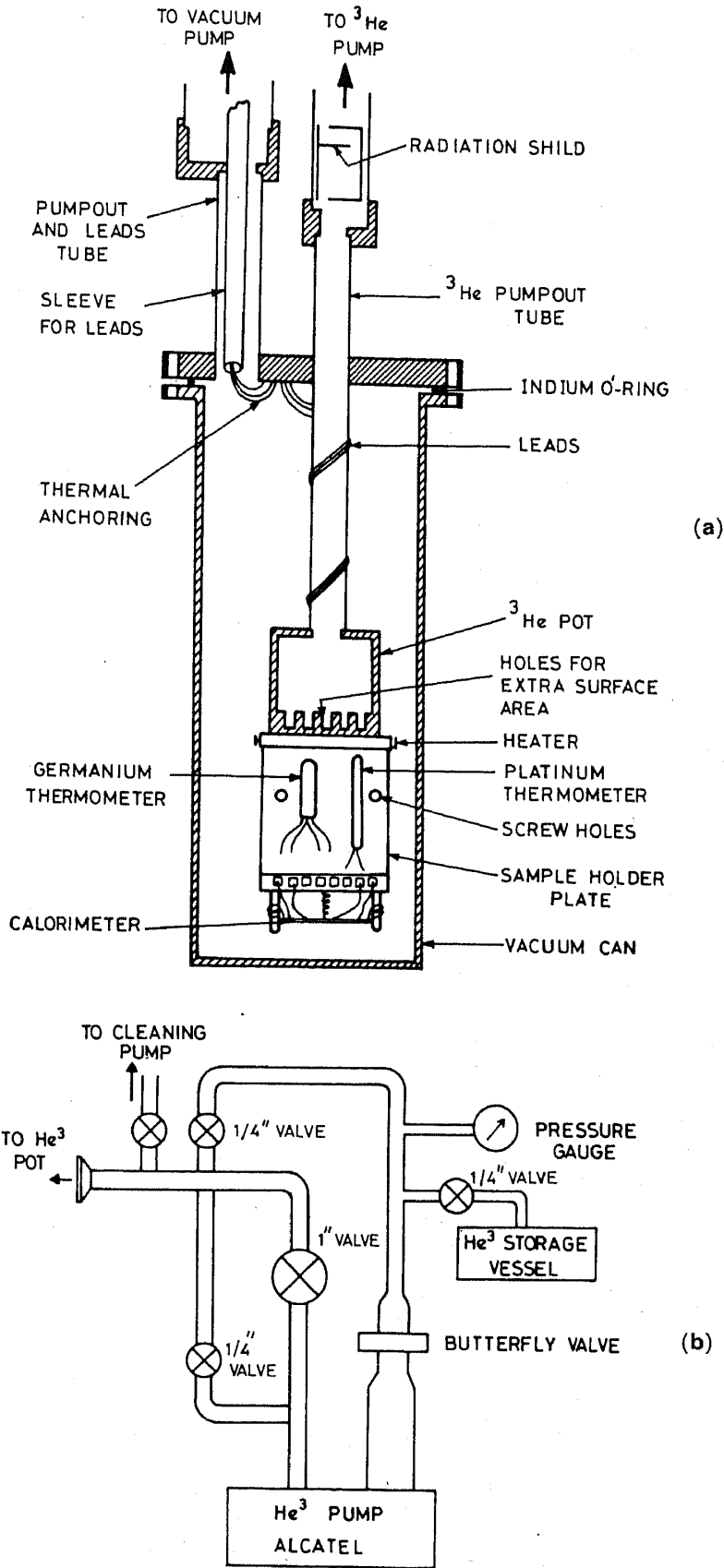


Figure 5. Schematic of He³ (a) cryostat and (b) gas handling system.

The gas handling system shown in figure 5(b) contains the pumping manifold, bellow sealed valves, a stainless steel gas storage vessel (made from a 5 litre stainless steel milk pot) and a hermetically sealed He^3 pump (586 l/min capacity). Except the bellow sealed valves (Nupro), sealed He^3 pump (Alcatel model 2033 H) and He^3 gas, rest of the materials are all locally available. The He^3 cryostat is a general purpose cryostat and can accommodate many different types of experiments. The thermal anchor of the calorimeter is tightly screwed to the cold finger connected to the base of the He^3 evaporator.

3.3 Electronics

The schematic of the electronics is shown in figure 6. The electronics is interfaced to a PC/XT via GPIB board. The software for control and data acquisition are written in GWBASIC or PASCAL. The details of the software are given in appendix.

The base temperature (T_B) is measured by a commercially calibrated Ge thermometer which is monitored by a conductance bridge whose output is recorded by a DMM. The output of the conductance bridge is put to a home-made PID controller for temperature control.

The resistance and hence the temperature of the sample thermometer (T_s) is measured by a simple AC technique using a lock-in amplifier (PAR 5204). The current through the thermometer is monitored separately by another DMM. The output of the lock-in needs to be recorded as a function of time to capture the ($T-t$) curve. We do that by using a system DMM (Keithley 193A). The ($T-t$) curve typically contains 300 data points recorded at (0.1–0.3)s intervals [The total length of wait time between two current steps is (5–10) τ]. We use the buffer of 193A for storage which is then transferred to the computer through GPIB interface after the complete ($T-t$) curve is recorded. This method of initial storage in the buffer allows rapid data acquisition and the speed

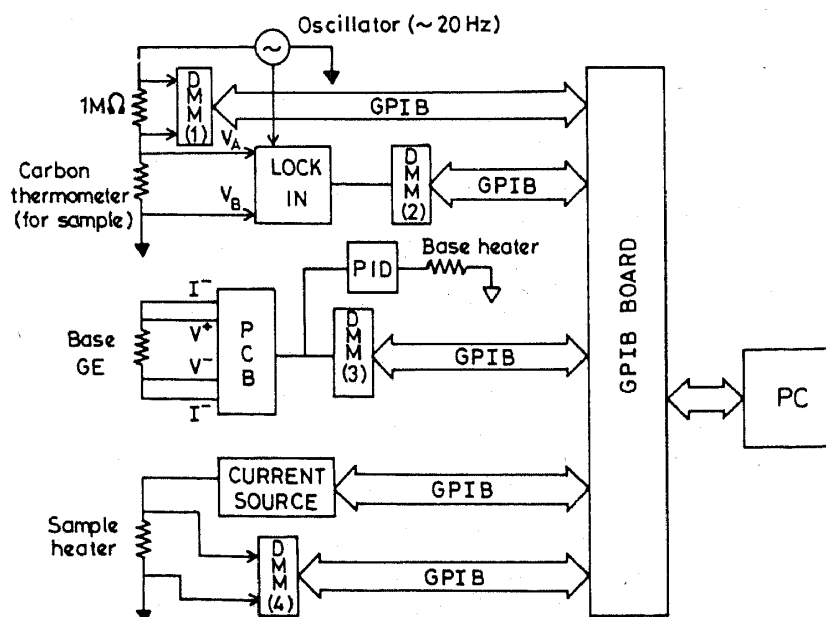


Figure 6. Instrumentation block diagram (DMM: Digital multimeter, PCB: Potentiometer conductance bridge, PID: Temperature controller.)

of data transfer through the GPIB interface does not come in the way of fast storing of the $(T - t)$ curve.

The current input to the heater ($5 \mu\text{A}$ – $300 \mu\text{A}$) is done by a programmable current source (Keithley 220). The heater resistance is essentially temperature independent. It is $2.474 \text{ k}\Omega$ at room temperature, $2.358 \text{ k}\Omega$ at 4.2 K and it stays constant within one part in thousand below 4.2 K .

4. Procedure for data taking and evaluation

The sample can be of arbitrary shape but should have one face well polished for thermal contact. A thin layer of Apeizon N grease is used for thermal contact with the calorimeter plate. The sample is weighed before putting it in the calorimeter. After mounting the sample, the calorimeter chamber is sealed with indium O-ring pumped down to 10^{-5} torr. After pumping, the vacuum chamber is isolated. After transfer of liquid nitrogen the cryostat cools to $\approx 80 \text{ K}$ in 6–8 h. The liquid helium is then transferred. The amount of liquid helium is around 10 litres including pre-cooling. During this period the He^3 evaporator is connected to the storage vessel. After the cool down to 4.2 K , the electrical checks are made and the bath is pumped down to 1.5 K . This condenses He^3 in the evaporator as seen by fall in storage vessel pressure. After the He^3 has condensed (in 90 min), the evaporator is pumped through the manifold till a temperature of 0.4 K is reached. The PID temperature is turned on to stabilize the base temperature around 0.45 K . Once the base temperature is stabilized (typically takes a minute or two), the specific heat measurement program is turned on. The measurement is done completely by the computer. The program, after checking the initial temperature gives a current step and triggers the 193A to monitor the sample temperature T as a function of time. After monitoring the sample temperature (for 30–50 s, for samples with small heat capacity, for 200–300 s, for sample of large heat capacity) the buffer of 193A is closed for data intake and is transferred to the computer disc for storage. After this a new trigger initiates a new current step and the data cycle starts. Typically from the lowest temperature ($\approx 0.5 \text{ K}$) to the highest temperature ($\approx 9.6 \text{ K}$) about 20–40 data points are taken. If the sample heat capacity is small so that the time between the currents steps are 30–50 s a number of heating and cooling cycles can be done within 3–4 h, the time over which the He^3 last in the evaporator.

5. Analysis of data, important numbers and illustrative number

The precision as well as accuracy of the heat capacity data depends on the accuracy with which the following quantities are determined:

- (1) The temperature calibration of the sample thermometer (i.e. resistance (R) vs T curve) and noise in the polynomial fit of R vs T curve. As a rule of thumb if ΔT , the step size is 10% of T and we want a "noise" in C determination less than 2%, the noise in the polynomial fit should be better than 0.2%.
- (2) The time constants τ at each temperature steps determined from $(T - t)$ curves using (5).
- (3) The effective thermal conductance \bar{K} of the link. In addition, the accuracy of the

results also depend on the reproducibility and stability of the thermometer calibration and that of the empty calorimeter heat capacity.

In the following we present some important numbers which serve as important diagnostics of the calorimeter performance. In figure 7 we have shown the \bar{K} as a function of T . Data from two runs with and without sample are shown to show its reproducibility. An estimate of \bar{K} can be obtained from thermal conductivity of copper. The thermal conductivity of Cu wire used was estimated from Wiedemann–Franz law (Ashcroft and Mermin 1976). The observed \bar{K} is somewhat lower than the estimated \bar{K} because of the thermal boundary resistance (Anderson and Peterson 1970). For the purpose of evaluation of $C(T)$ we make a spread sheet of \bar{K} and T from the experimental data.

Next step in the analysis is to find $\tau(T)$ from the set of $(T - t)$ curve obtained at each step. The τ can be obtained by a non-linear least square fit data to (5). A typical data and fit are shown in figure 8(a). Alternatively τ can also be obtained from a linear fit to T vs dT/dt as shown in figure 8(b). The later method is also a check that $(T - t)$ curve follows a single exponential. τ determined by both methods agree to within 5%. The τ as a function of temperature is shown in figure 9. The τ 's for empty calorimeter as well as those with Cu sample are shown. Since \bar{K} is sample independent, the specific information about C is contained in τ .

After the $(T - t)$ scans for each current step are stored in the computer and analysed to obtain τ , a column of τ is added to the already existing spread sheet containing \bar{K} and T . [Since both \bar{K} and τ refer to the average temperature of a step, temperature where τ and \bar{K} are both determined is the same for a given step] from this spread sheet the total heat capacities C as a function of T are determined. The measured empty calorimeter heat capacity is then subtracted and one obtains the heat capacity of the sample. As an illustrative example we show these heat capacities in figure 10 for a run with 420 mg of ordinary machine shop Cu. At 1 K, the heat capacity of copper is approximately a

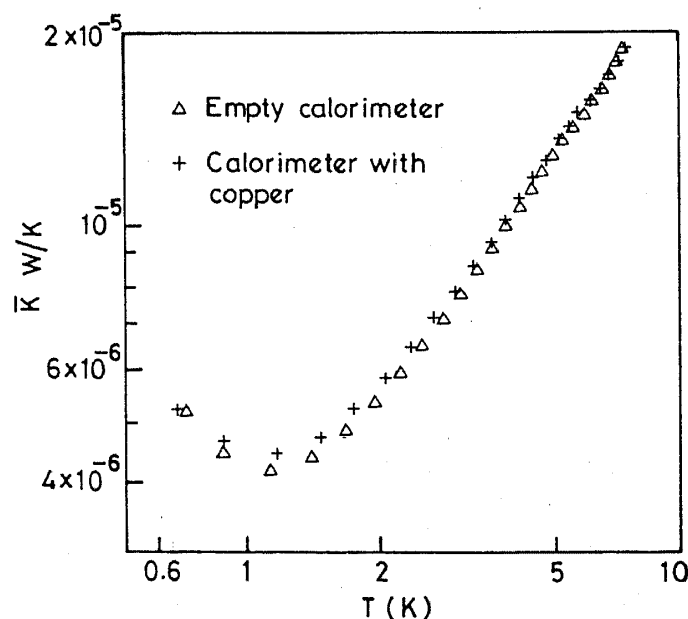


Figure 7. Thermal conductivity \bar{K} as a function of temperature for empty calorimeter (Δ) and with copper sample (+).

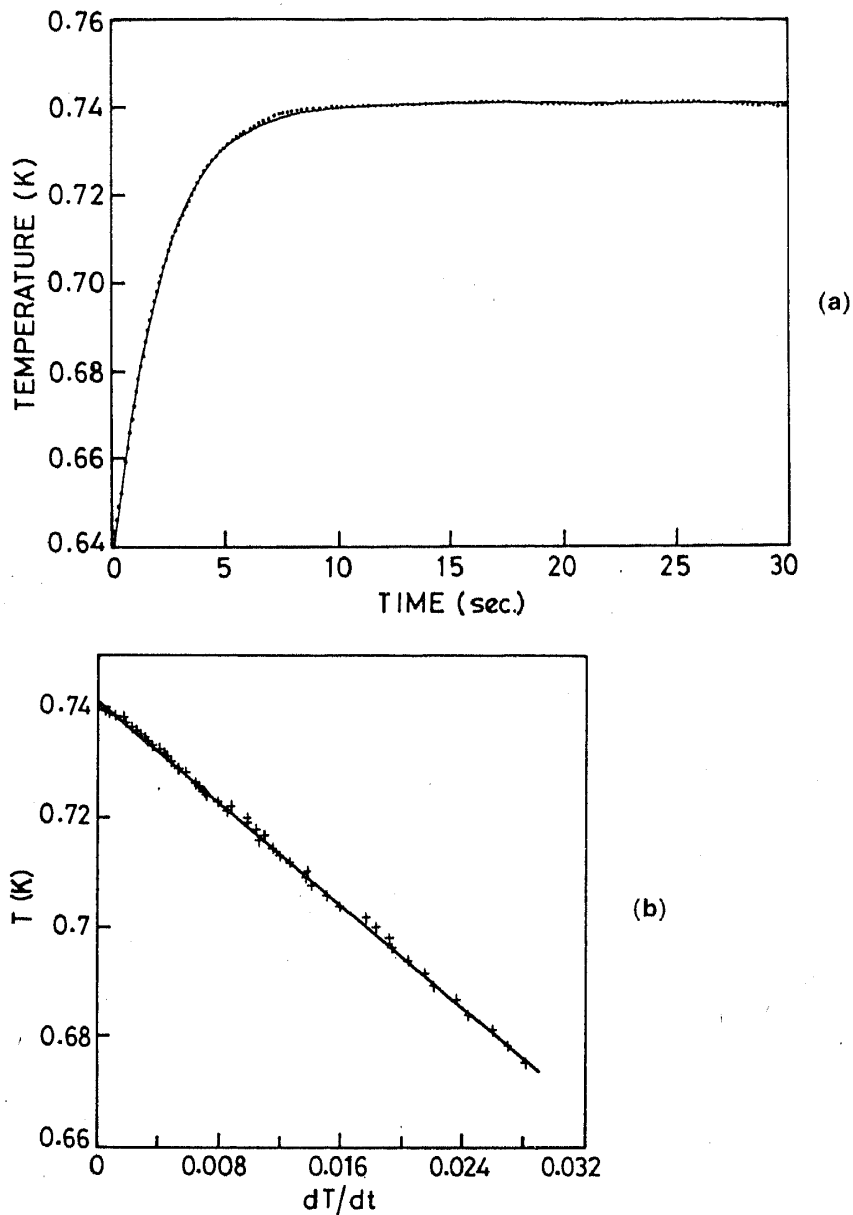


Figure 8. (a) A typical data and non-linear square fit to equation (5) to obtain τ . (b) T vs dT/dt , τ can be obtained from a linear fit.

factor of two more than that of the empty calorimeter. The main contribution to the empty calorimeter heat capacity arises from the carbon thermometer, the copper leads to the carbon thermometer and the sapphire base. Small contributions also come from glues and grease and the metal films. The Cu, an often quoted standard, shows the specific heat $C_p = \gamma T + \delta T^2$ we obtain $\gamma = 0.600 \text{ mJ}/(\text{K}^2 \text{ g at})$ and $\delta = 0.0475 \text{ mJ}/(\text{K}^4 \text{ g at})$ (see Schulz 1974 and Regelsberger 1986) accepted γ is $0.672 \text{ mJ}/(\text{K}^2 \text{ g at})$ in Ashcroft and Mermin 1976 (table 2.3).

In figure 11 we show the specific heat of aluminium (361 mg) measured near superconducting transition temperature T_c . The data are shown as C_s/C_n and as a function of T/T_c . The discontinuity in specific heat at T_c , $(C_s - C_n)/C_n \approx 1.4$ is close to the value obtained by Phillips (1959). The T_c observed by us from the specific heat jump

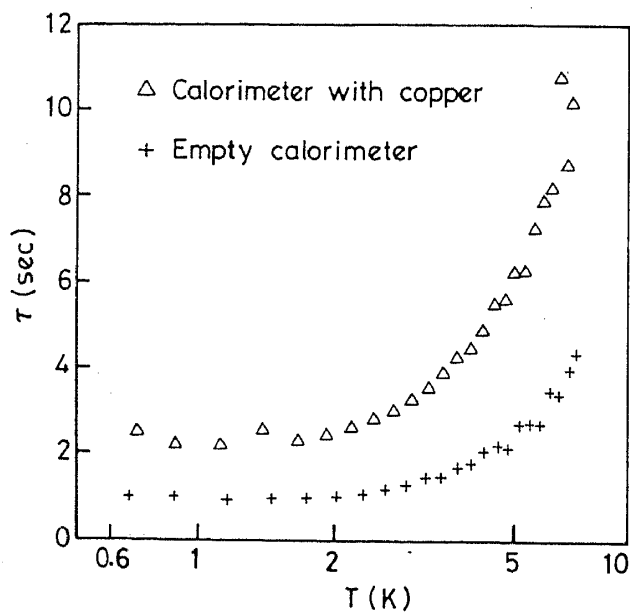


Figure 9. τ as a function of temperature for empty calorimeter (+) and with copper sample (Δ).

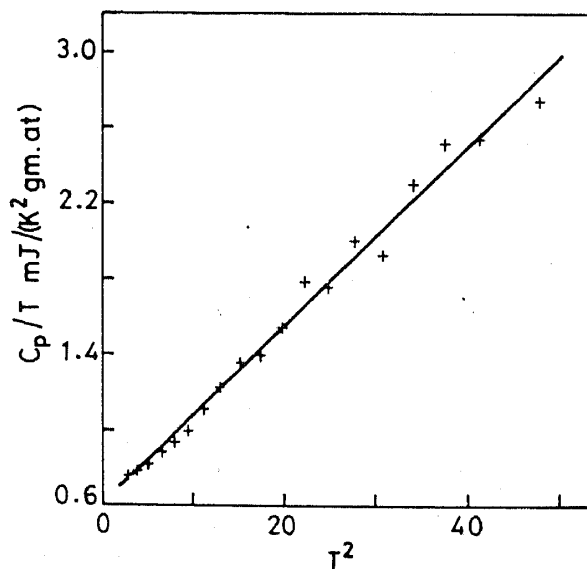


Figure 10. Specific heat for copper (420 mg) sample.

is about 5% more than the accepted T_c of aluminium. This we suspect is due to finite step size of the temperature used.

Conclusion

In this paper we described a simple automated system in which one can measure specific heats of solids below 10 K. At present our accuracy is not very high. However, this may be an acceptable accuracy in many studies. The low accuracy arises mainly

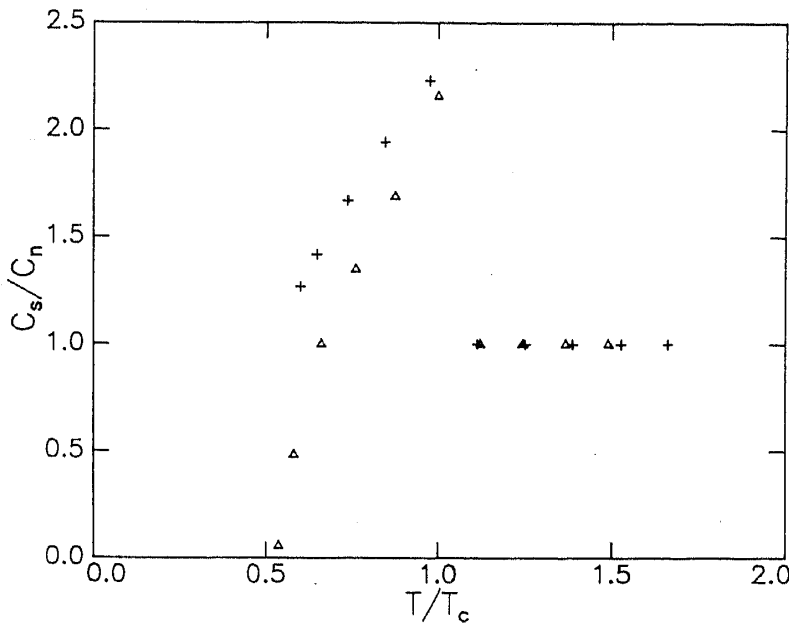
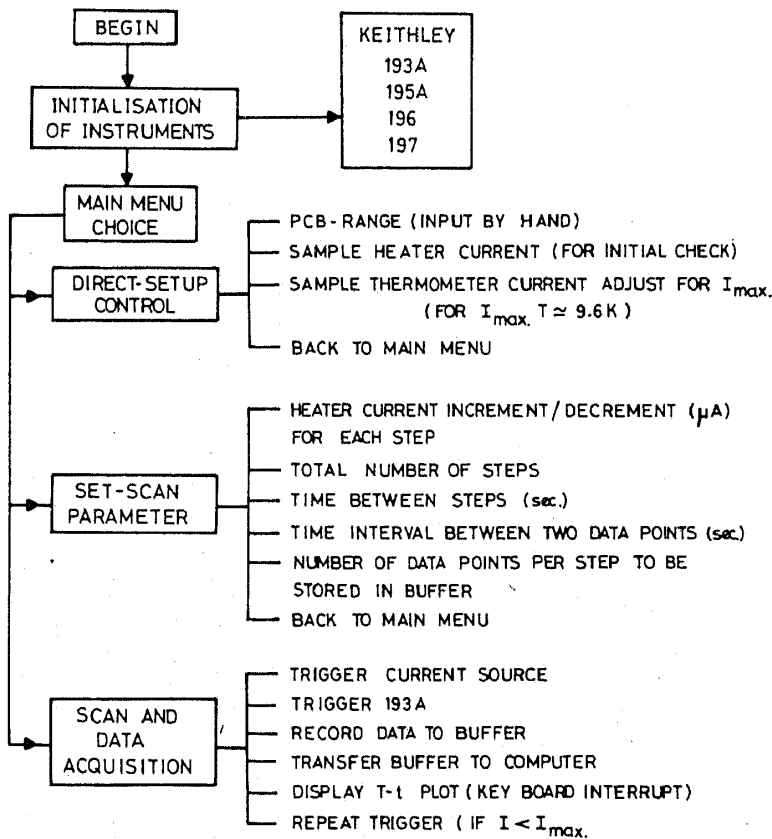


Figure 11. C_s and C_n are specific heats of aluminium in superconducting and normal state respectively. $(C_s - C_n)/C_n = 1.4$, data are compared with that of N E Phillips (+) (Phillips 1959).

from the thermometer which needs some what better calibration as well as fitting procedure. Work is underway to remedy these defects.

Appendix



Acknowledgement

The work is supported by CSIR in the form of a sponsored scheme.

References

- Anderson A C and Peterson R E 1970 *Cryogenics* **10** 430
Ashcroft N W and Mermin N D 1976 *Solid State Physics*, (New York: Hold-Saunders International Editions)
Bachmann R, DiSalvo Jr F J, Geballe T H, Howard R E, King C N, Kirsh H C, Lee K N, Schwall R E, Thomas H U and Zubeck R B 1972 *Rev. Sci. Instrum.* **43** 205
De Puydt J M and Dahlberg E D 1986 *Rev. Sci. Instrum.* **57** 483
Dutzi J, Pattalwar S M, Dixit R N and Shete S Y 1988 *Pramana - J. Phys.* **31** 253
Lakshmikumar S T and Gopal E S R 1981 Recent development in the technique of heat capacity measurement. NTPP-PHY-3, IISc, Bangalore
Phillips N E 1959 *Phys. Rev.* **114** 676
Raychaudhuri A K 1980 *A search for low temperature in glasses* Ph.D. Thesis, Cornell University
Regelsberger M, Wernhardt R and Rosenberg M 1986 *J. Phys.* **E19** 525
Schultz R J 1974 *Rev. Sci. Instrum.* **45** 548
Stewart G R 1983 *Rev. Sci. Instrum.* **54** 1
Shepherd John P 1985 *Rev. Sci. Instrum.* **56** 273